Pergamon

Int. J. Heat Mass Transfer. Vol. 40, No. 14, pp. 3335–3349, 1997

Printed in Great Britain
0017–9310/97 $17.00+0.00

PII: S0017-9310(96)00373-0

Time-averaged and reverse transition in oscillatory air convection in a differentially heated rotating cubic cavity

Y. T. KER and T. F. LIN†

Department of Mechanical Engineering, National Chiao Tung University, Hsinchu, Taiwan, Republic of China

(*Received* 31 *July* 1996 *and in final form* 1 *November* 1996)

Abstract—An experimental study was carried out to investigate the time-averaged and unsteady thermal characteristics in an inclined cubic air cavity, subject to differential heating across a pair of side walls and subject to rotation about an axis which is normal to the insulated bottom wall and through the geometric center of the cavity. Specifically, the air temperature in the cavity at selected locations was measured for both steady and unsteady flows. Results were obtained for the cavity height $H = 10$ and 15 cm, temperature difference ΔT ranging from 2 to 10°C, rotation rate Ω from 0 to 452.9 rpm and inclined angle ϕ from 0 to 90° (heated from below). Time records of the air temperature showed the presence of the flow re-stabilization in two different ranges of the rotation rates. Thus, the transient oscillatory flow can be stabilized by increasing the cavity rotation when the rotation rate is in these ranges. This flow restabilization is more pronounced for a higher inclined angle. Moreover, a power spectrum density analysis of the time records indicated that at low rotation rates the amplitudes of the temperature oscillation are location dependent, but the oscillation frequencies at various locations for a given set of ΔT, Ω and ϕ are the same.

1. INTRODUCTION

In growing high purity bulk crystal and thin crystal film for various semiconductor applications, crucibles are often rotated to suppress thermal buoyancy induced velocity and temperature oscillations in the fluid phase and to obtain spatially uniform solidification or deposition rate of the solid phase, but details on the complex flow driven by the simultaneous presence of the thermal buoyancy and rotation induced Coriolis and centrifugal forces are still poorly understood. To unravel this complex flow, the present authors [1] recently carried out a numerical simulation to parametrically illustrate the effect of each individual driving force on the flow structure in a rotating cubic air cavity subject to differential heating across a pair of opposite side walls. Then in a following study [2] the steady flow, driven by the thermal buoyancy and rotation induced interactive driving forces, was numerically investigated along with some measured data for the time variations of the air temperature for $H = 10$ cm. The data clearly showed flow stabilization by cavity rotation when the rotation rate was low. However, the flow becomes unstable at high rotation rate. Extension is made in the present study to measure more data for a wider range of the thermal Rayleigh number Ra, rotational Rayleigh number Ra_Ω and Taylor number Ta for two cavities ($H = 10$ and 15 cm), intending to find the possible presence of different flow stabilization characteristics. In addition, oscillation frequencies of the temperature data are calculated by a power spectrum analysis to delineate detailed fluctuating characteristics of the flow.

Considerable attention was paid in the earlier study to convection in a bottom heated, horizontal fluid layer, rotating at a constant angular speed about a vertical axis [3–9]. Niller and Bisshopp [3] noted from stability analysis that in the limit of a large Taylor number Ta viscous effects play an important role in a thin layer near the boundary and the critical Rayleigh number Ra_C for the onset of convection is independent of whether the boundaries are rigid or free. Numerical analysis from Veronis [4] indicated that the Prandtl number Pr exhibits significant effects on the flow and thermal structures. For the limit of infinite Prandtl number Küpper and Lortz [5] showed that no stable steady-state convective flow exists if the Taylor number exceeds a certain critical value given in their study. Rossby [6] experimentally observed the subcritical instability in a water layer for $Ta > 5 \times 10^4$ and in a mercury layer for $Ta < 10^5$. In addition, for water at $Ra > 10^4$ the Nusselt number was found to increase with the Taylor number. The trend is opposite for mercury. Furthermore, at a large Taylor number oscillatory convection is preferred in mercury. Based on a mean-field approximation, Hunter and Riahi [7] analytically showed the nonmonotonic variation of Nusselt number with Taylor number. Linear stability analysis from Rudraiah and Chandna [8] indicated

† Author to whom correspondence should be addressed.

NOMENCLATURE

f	frequency
g	gravitational acceleration
H	length of cavity
PSD	power spectrum density
Ra	Rayleigh number, $\beta g \Delta T H^3/\alpha\nu$
Ra_C	critical Rayleigh number
Ra_Ω	rotational Rayleigh number, $\beta\Omega^2\Delta T H^4/\nu\alpha$
t	time
T	local temperature
Ta	Taylor number, $\Omega^2 H^4/\nu^2$
T_H	temperature of the hot wall
T_L	temperature of the cold wall
x, y, z	dimensional coordinate systems
X, Y, Z	dimensionless coordinate systems scaled with H.

Greek symbols

α	thermal diffusivity
β	thermal expansion coefficient
ΔT	temperature difference between the hot and cold walls, $T_H - T_L$
θ	dimensionless temperature $(T-T_L)/(T_H-T_L)$
θ_{av}	nondimensional time-averaged temperature
ν	kinematic viscosity
τ	dimensionless time, $t/(H^2/\alpha)$
ϕ	inclined angle between the gravity and rotating axis
Ω	magnitude of rotating rate.

that the critical Rayleigh number was relatively sensitive to the method and rate of heating, Coriolis force and the nature of the surfaces bounding the fluid layer. The analysis from Clever and Busse [9] suggests that the critical Rayleigh number for the onset of oscillatory motion is higher for higher Taylor and Prandtl numbers.

Another geometry of considerable interest is the flow in a bottom heated vertical closed circular cylinder rotating about its own axis. Experiments for silicone oil carried out by Hudson and his coworkers [10, 11] indicated that the Nusselt number increases with rotation rate. A steady axisymmetric numerical simulation was carried out by Chew [12]. The onset of steady natural convection was shown by Buell and Catton [13] to be sensitive to lateral thermal boundary condition. Pfotenhauer *et al.* [14] reported the effects of cylinder geometry on the onset of convection for low temperature liquid helium. For water subject to high Rayleigh and Taylor numbers, Boubnov and Golitsyn [15] experimentally observed a ring pattern of convective flow resulting from the fluid spin-up and vortex interactions between two adjacent vortices. Kirdyashkin and Distanov [16] found that a periodically changing rotation speed can result in periodical temperature changes throughout the entire liquid layer.

Experimental data for the Nusselt number in a top heated horizontal rectangular cavity of silicone oil rotating about a vertical axis passing through the geometric center of the cavity were presented by Abell and Hudson [17]. Hathaway and Somerville [18] conducted a three-dimensional and unsteady numerical simulation of an inclined rotating layer, with the rotation vector tilted from the vertical. The tilting of the rotation vector was found to produce significant change in the flow structure. A combined theoretical, numerical and experimental study was presented by Bühler and Oertel [19] to investigate thermal convection in a rotating rectangular shallow box heated from below. First, linear stability analysis was used to predict the onset of steady and oscillatory convection and a three-dimensional flow configuration. Then, the numerical analysis predicted the change of the roll orientation with the Taylor number. Finally, the flow structures at various Rayleigh and Taylor numbers were visualized.

The above literature review indicates that the previous studies mainly focused on effects of rotation on the onset of convection and overall heat transfer at supercritical Rayleigh numbers. The detailed processes on how the rotation affects the flow stability and the unsteady flow characteristics are still not well understood. In this study, comprehensive temperature measurements were taken to investigate the effect of rotation on flow stabilization and to deduce fluctuating characteristics of the unsteady flow in a differentially heated, rotating, inclined cavity at higher thermal Rayleigh, rotational Rayleigh and Taylor numbers.

2. EXPERIMENTAL APPARATUS FOR TEMPERATURE MEASUREMENT

The experimental system for measuring the thermal characteristics in a rotating cubic air cavity schematically shown in Fig. 1 consists of four parts-rotating frame, test section, temperature control unit and temperature measuring unit. Figure 2 shows the details of the test section. Specifically, the cavity is rotated at a constant angular speed Ω about an axis which is parallel with the side walls and is through the center of the cavity. The rotating axis inclines from the vertical by an angle ϕ.

The rotating frame is made up of a rotary table of 31.5 cm in diameter and is mounted on a steel shaft

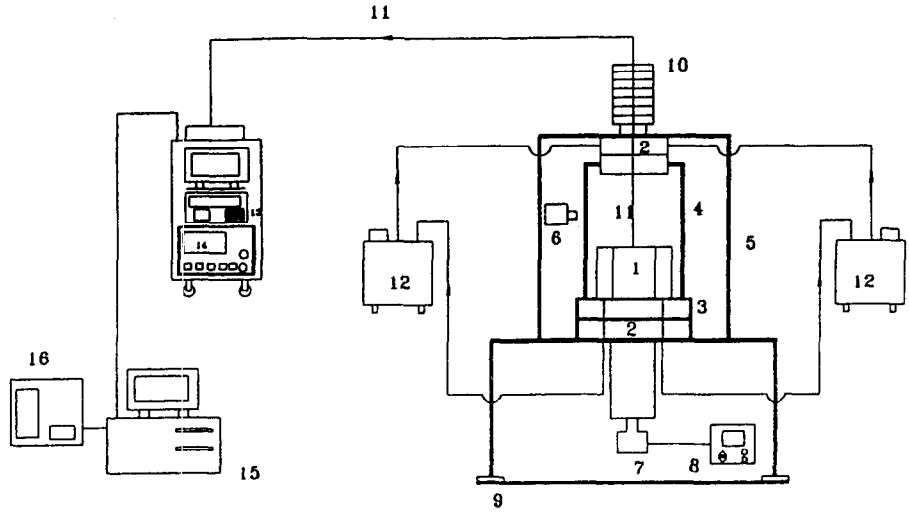

1 : test section
2 : fluid slip ring
3 : supporting frame
4 : rotating frame
5 : statatic frame
6 : photo - electric tachometer
7 : 2 hp induction motor
8 : inverter
9 : platform
10 : slip ring
11 : thermocouples
12 : thermostat
13 : data acquisition system
14 : digital multimeter
15 : PC computer
16 : laser printer

Fig. 1. Schematic diagram of the experimental system.

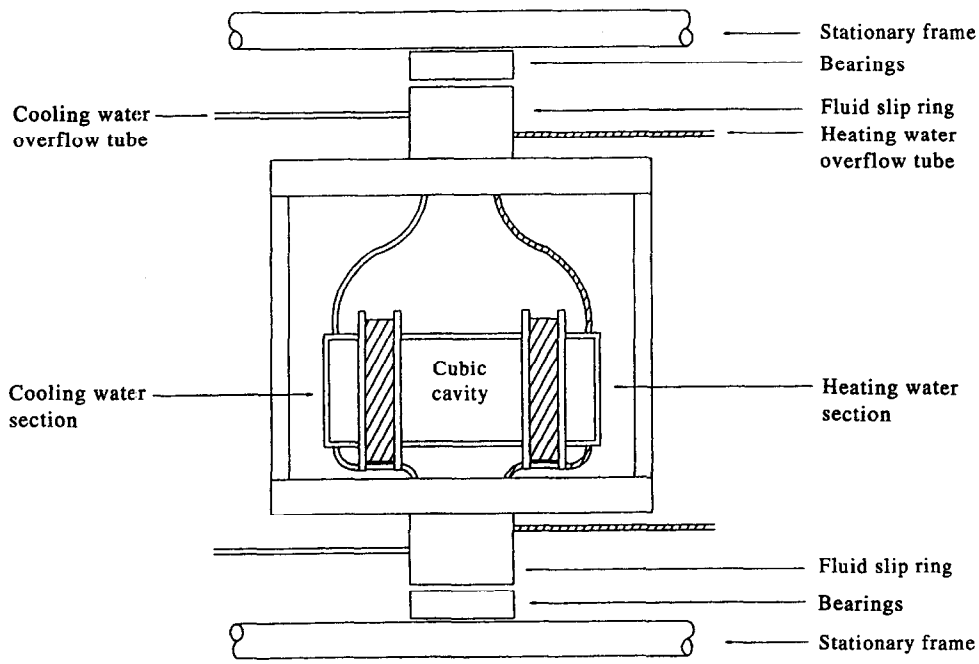

Fig. 2. Rotating assembly.

Table 1. Uniformity of the isothermal walls without rotation for the cavity height $H = 10$ cm

Location (X, Y, Z)	T_L (°C)	Location (X, Y, Z)	T_H (°C)
0.5, 0.355, −0.355	15.05	−0.5, −0.355, −0.355	35.07
0.5, 0.0, −0.355	15.04	−0.5, 0.0, −0.355	35.15
0.5, −0.355, −0.355	15.02	−0.5, 0.355, −0.355	35.14
0.5, 0.355, 0.0	15.04	−0.5, −0.355, 0.0	35.09
0.5, 0.0, 0.0	15.00	−0.5, 0.0, 0.0	35.13
0.5, −0.355, 0.0	15.01	−0.5, 0.355, 0.0	35.10
0.5, 0.355, 0.355	14.92	−0.5, −0.355, 0.355	34.98
0.5, 0.0, 0.355	14.95	−0.5, 0.0, 0.355	35.02
0.5, −0.355, 0.355	14.90	−0.5, 0.355, 0.355	35.00

of 3 cm in diameter. The frame is designed to provide a space of 27.6 cm in diameter and 27.3 cm in height for housing the test section. The shaft is rotated by a 2 hpower d.c. motor with its speed controlled by an inverter and the rotation speed is detected by a photoelectric tachometer. Care is taken to ensure that the table rotates centrally and steadily.

The test section fixed on the rotating table is a cubic air enclosure of 10 or 15 cm in length. Two opposite walls of the cavity made of 2.5 mm thick copper plates are controlled at uniform but different temperatures by circulating constant temperature coolants through them. Two fluid sliprings are used to allow coolants to pass from the stationary thermostats to the rotating cavity. The thermostats used are LAUDA RK-20 compact constant temperature baths with a temperature range of −40 to 150°C and a resolution of 0.1°C. Care must be taken to prevent coolant leak from the fluid sliprings. The other walls are made of 10 mm thick acrylic plates and thermally insulated by super-lon foam. With this arrangement the temperature uniformity of the isothermal plates can be controlled to within ±0.1°C. The sampled measured data for the temperature of the hot and cold walls at selected locations are given in Table 1.

Thermocouple connections are arranged differentially for the stationary and rotating cavities. For the limiting case of a non-rotating cavity 27 T-type thermocouples are placed in the cavity and are connected directly to an external circuit. While in the rotating cavity the thermocouples are fixed at the designated locations by high performance fine Neoflon thread, which is in turn fixed across a pair of opposite side walls. Prior to installation the thermocouples are calibrated by the LAUDA thermostats and high precision liquid-in-glass thermometers. Voltage signals from the thermocouples are passed through a slip ring to the HP 3852A data acquisition/control system and then to a personal computer for further data processing. Data collection is normally started when the flow already reaches steady or statistically steady state. In view of the low speed flow in a rotating cavity, velocity measurements are difficult and were not conducted in the study.

The test is started by first setting the temperature of the thermostats at predetermined values and then recirculating coolants through the isothermal walls of the rotating cavity. The average value of the hot and cold plate temperatures is adjusted to be approximately equal to the ambient temperature, so that heat loss from the cavity to the ambient can be reduced and thermal radiation across the plates is minimized. In the meantime the cavity is rotated at the predetermined speed. Then the air temperature inside the cavity is measured at selected locations. After the transient stage has elapsed, the temperature data are stored and analyzed.

The ranges of the governing parameters to be investigated are as follows: the rotating speed varied from 0 to 452.9 rpm, the inclined angle from 0 to 90° and the temperature difference across the cavity from 2 to 10°C for two cubic cavities of $10 \times 10 \times 10$ cm^3 and $15 \times 15 \times 15$ cm^3. The uncertainty analysis of the measurement is summarized in Table 2.

3. RESULTS AND DISCUSSION

In the following only a small sample of the results obtained from the present study will be presented to illustrate the steady and time dependent thermal

Table 2. Summary of uncertainty analysis

Parameters	Uncertainty
H (m)	±0.00025 m
T_H, T_L	±0.1°C (non-rotating)
T_H, T_L	±0.2°C (rotating)
T (thermocouples)	±0.05°C
α (m^2/s)	±0.07%
β (K^{-1})	±0.05%
ρ (Kg/m^3)	±0.05%
ν (m^2/s)	±0.07%
Ω (rpm)	±0.3%
ϕ (degree)	±0.25°
Ta	±10.5%
Ra	±8.5%
Ra_Ω	±11.5%

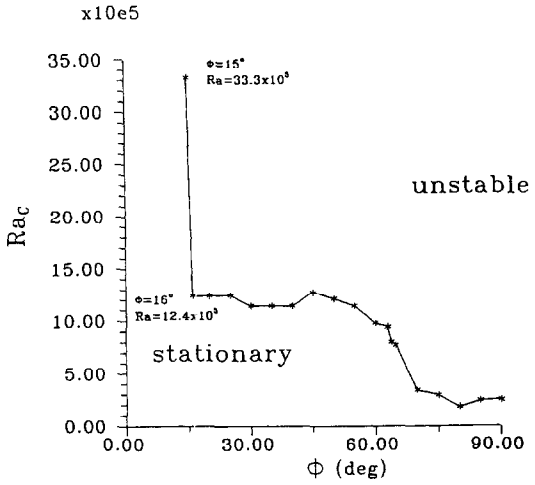

Fig. 3. Variation of critical Rayleigh number for onset of time dependent temperature oscillations with the inclined angle for a non-rotating cavity with $H = 15$ cm.

characteristics in an air cavity which is inclined at an inclined angle, rotated at various rotation rates and subject to various temperature differences.

Before presenting results for the rotating cavity, the effect of cavity inclination on critical Rayleigh number Ra_C for the air temperature to change from the steady to the time dependent state for the limiting case of zero rotation rate ($\Omega = 0$) is first examined in Fig. 3. The results indicate that in the range of the Rayleigh number studied here ($1.0 \times 10^5 < Ra < 5 \times 10^6$) the flow is always steady for ϕ up to 14°. At $\phi = 15°$ Ra_C is at 33.3×10^5. There is a sudden drop in the critical Rayleigh number for ϕ raised from 15 to 16°. The physical background on the existence of this drastic change in Ra_C is not known and requires further investigation. For $16° \leqslant \phi \leqslant 45°$ the critical Rayleigh number is around 1.2×10^6. Reduction in Ra_C is noted for $45° < \phi < 80°$. Ra_C stays nearly at 2.5×10^5 for $80° \leqslant \phi \leqslant 90°$.

To investigate the influence of inclined angle and rotation speed on the thermal characteristics in the cavity and to provide some data for verifying numerical computation, the time-average air temperature variations with the space coordinate X were measured. The coordinate system is chosen to rotate with the cavity with its origin at the geometric center of the cavity. Specifically, the X-, Y- and Z-axes are, respectively, normal to the isothermal side, insulated side and top walls. Figure 4(a)–(d) present these data along the X-axis through the origin for the various ϕ and Ω at $\Delta T = 10$°C with $H = 15$ cm. These results indicate that in a non-rotating cavity ($\Omega = 0$) the measured air temperatures at the same location for various inclined angles deviate only slightly except in the regions near the isothermal side walls. Additionally, on the isothermal walls the temperature gradients in the X-direction inferred from the data in Fig. 4(a) are highest for the cavity with $\phi = 60°$. It is known that the heat transfer in a non-rotating cavity is dominated by the thermal buoyancy driven, main flow recirculation rising along the hot wall and sinking along the cold wall. Thus the temperature gradients evaluated from Fig. 4(a) can reflect the trend of heat transfer for various ϕ. Hence the present data suggest that heat transfer is highest for $\phi = 60°$ and lowest for $\phi = 90°$. This is in good agreement with our previous three-dimensional computation [20]. As the cavity is rotated at 30.8 rpm, the associated Coriolis force ($Ta = 2.34 \times 10^7$) and centrifugal buoyancy ($Ra_\Omega = 5.06 \times 10^6$) are large enough to induce strong cross plane secondary flow [2]. This secondary flow strongly interacts with the thermal buoyancy driven flow which is relatively sensitive to the cavity inclination [20]. The resulting temperature fields also become sensitive to the inclined angle, as evident from the data in Fig. 4(b). For a rise of rotation rate to 45.3 rpm, the rotation driven secondary flow gets stronger and the thermal characteristics in the cavity flow depend less on the inclined angle. This is clear when the data in Fig. 4(c) are compared with those in Fig. 4(b). It is of interest to note that at an even higher rotation speed of 97.4 rpm ($Ta = 2.34 \times 10^8$, $Ra = 3.18 \times 10^6$, $Ra_\Omega = 5.06 \times 10^6$) the rotation driven flow dominates over the buoyancy driven flow so that the cavity inclination produces little effect on the temperature variation (Fig. 4(d)). It should be mentioned that the cross plane secondary flow is rather strong for $\Omega \geqslant 30.8$ rpm and the heat transfer coefficient has complex distributions on the isothermal walls [1]. Thus the calculated temperature gradients on the isothermal walls for $\Omega \neq 0$ do not represent the general trend of the heat transfer affected by ϕ and Ω.

Typical results to illustrate the effects of the rotation rate on the air temperature distribution are shown in Fig. 5 for $\Delta T = 10$°C ($Ra = 9.43 \times 10^5$) and 4.6°C ($Ra = 4.36 \times 10^5$) at $\phi = 0°$ for various Ω with $H = 10$ cm. The results in both Fig 5(a) and (b) indicate that at a low rotation rate ($\Omega \leqslant 45.3$ rpm, $Ta \leqslant 1.0 \times 10^7$) the cavity rotation exhibits profound effects on the temperature variation. For a higher Ω the rotation effects diminish gradually. In fact, as $\Omega \geqslant 307.9$ rpm ($Ta \geqslant 4.62 \times 10^8$) the measured temperature data overlap. This is conjectured to result from large amplitude, highly chaotic fluctuation of the flow when it is subject to the high Coriolis and centrifugal forces at these high rotation rates. The flow can be considered to be at a fully turbulent state so that the temperature distributions become invariant with the X-direction.

The temporal stability of the air flow affected by cavity rotation is illustrated next by showing the measured time variations of the instantaneous air temperature at selected locations for various rotation rates and inclined angles. Figure 6 presents these data measured at location $(X, Y, Z) = (0.44, 0, 0)$ in a vertical cavity with $\phi = 0°$ for $\Delta T = 10°$ and 4.6°C for $H = 15$ cm. Since only the data at the statistically steady state are recorded, the nondimensional time

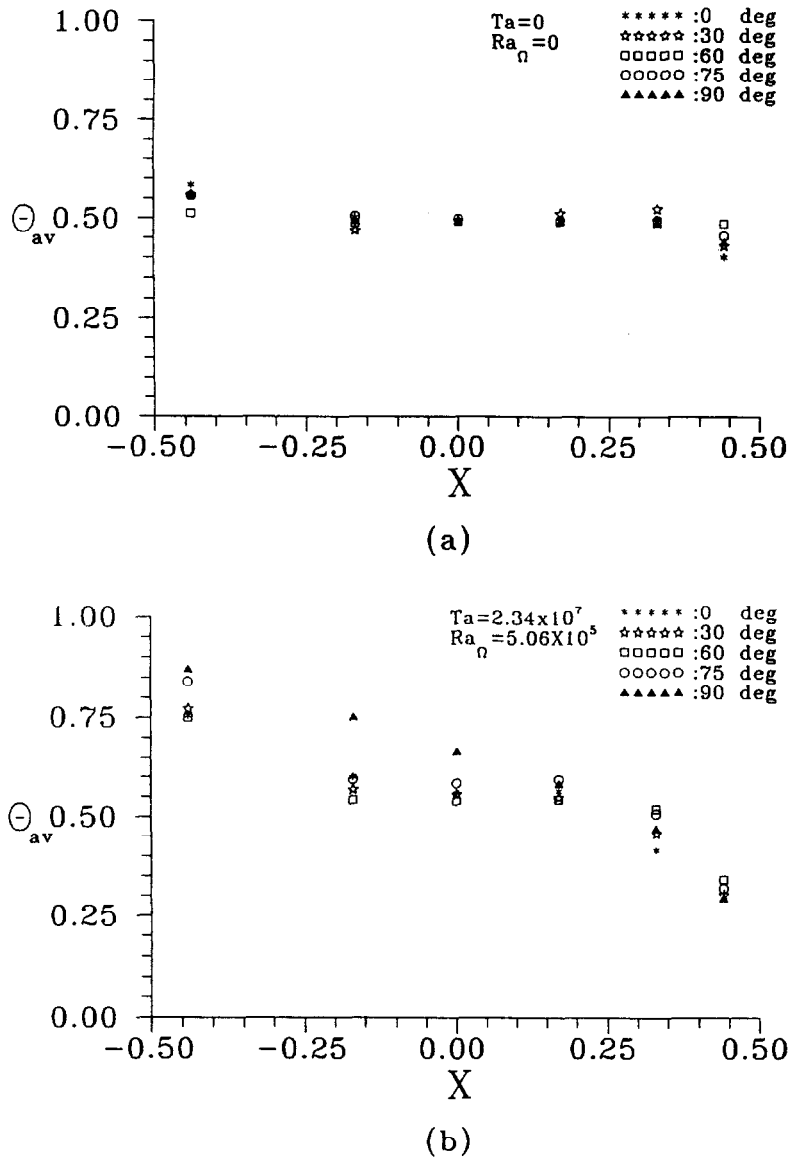

Fig. 4. Nondimensional time-averaged temperature distributions along X-axis for various inclined angles at $H = 15$ cm and $\Delta T = 10°C$ ($Ra = 3.18 \times 10^6$), for rotational rates: (a) $\Omega = 0$ rpm; (b) $\Omega = 30.8$ rpm; (c) $\Omega = 45.3$ rpm; and (d) $\Omega = 97.4$ rpm. (*Continued opposite.*)

$\tau = 0$ stands for a certain arbitrary selected time instant at that state. The results in Fig. 6(a) for $\Delta T = 10°C$ ($Ra = 3.18 \times 10^6$) at $\Omega = 0$ and 30.8 rpm show that relatively small amplitude, irregular temperature oscillations prevail in a non-rotating or slowly rotating cavity. The temperature oscillation amplitude is all less than 0.01 in a dimensionless unit or less than 0.1°C dimensionally. This small amplitude oscillation can be considered as resulting from the background noise always existing in the test apparatus and the flow can be regarded as steady. A rise of Ω to 45.3 rpm, however, causes a noticeable increase in the oscillation amplitude. It is interesting to note that a further raise of Ω to 97.4 and 143.2 rpm lowers the amplitude of the oscillation. In fact, the flow can be considered as steady for $\Omega = 143.2$ rpm. The oscillation amplitude, nevertheless, augments significantly when Ω is raised to 307.9 and 452.9 rpm. The above results clearly suggest that the cavity rotation introduces a nonmonotonic change in the oscillation amplitude at increasing rotation rate. Thus a rotation induced flow re-stabilization is found in the rotating

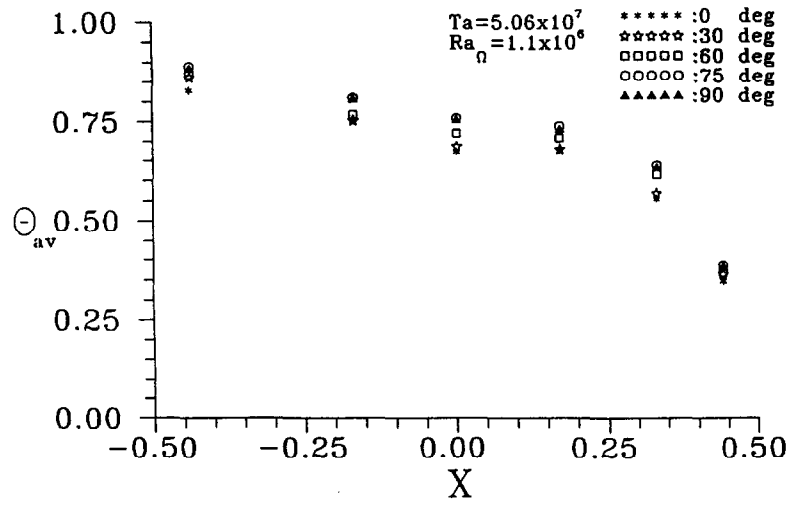

(c)

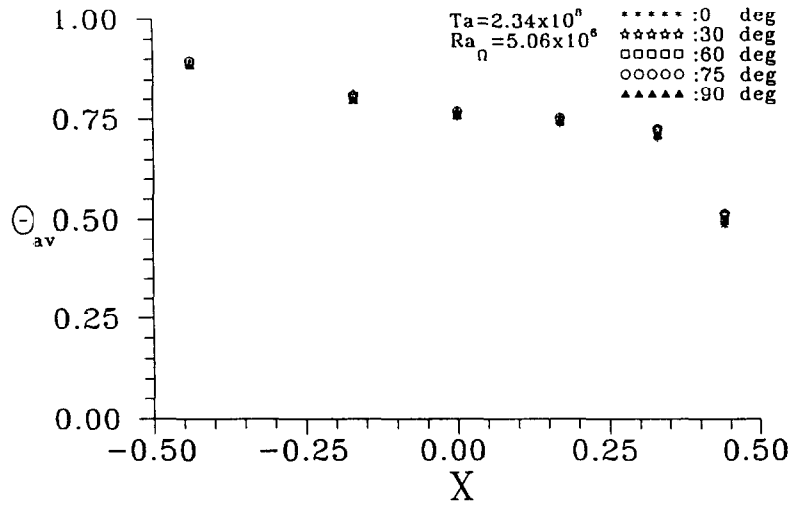

(d)

Fig. 4—*continued.*

cavity for $\Delta T = 10°C$ and $\phi = 0°$. Similar trends can be found for the effects of cavity rotation on flow stability for a lower thermal buoyancy at $\Delta T = 4.6°C$ shown in Fig. 6(b). The rotation induced flow re-stabilization in a slightly tilted cavity at $\phi = 30°$ resembles that in a vertical cavity ($\phi = 0°$) just discussed. As the inclined angle is increased to 60 and 75°, the flow restabilization driven by rotation becomes more pronounced when the results in Fig. 7 for $\phi = 60°$ and 75° with $H = 15$ cm are inspected. The results suggest that increase of Ω from 0 to 30.8 rpm, then to 45.3 rpm causes the flow to change from a chaotic state to quasi-periodic state, then to a steady state. At a further increasing rotation rate the flow goes to time periodic state and then back to a steady state at 143.2 rpm. At an even higher Ω the flow bifurcates again to a time periodic state and then to a chaotic state at $\Omega = 452.9$ rpm.

The space dependence of the flow oscillation is examined in Fig. 8 which displays the time histories of the air temperature at six selected locations for $\phi = 75°$, $\Omega = 30.8$ rpm and $\Delta T = 10°$ and 4.6°C for

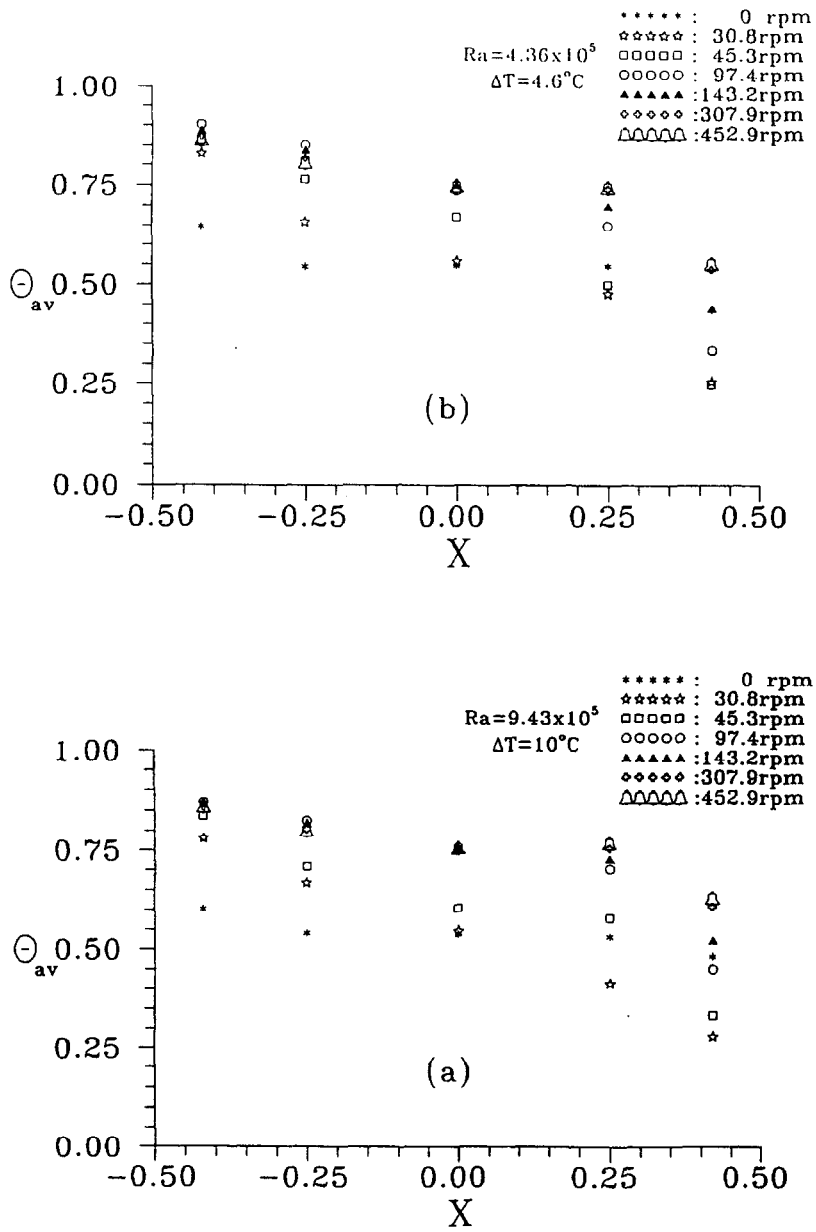

Fig. 5. Nondimensional time-averaged temperature distributions along the X-axis for various rotation rates at inclined angle $\phi = 0°$, $H = 10$ cm for (a) $\Delta T = 10°C$ and (b) $\Delta T = 4.6°C$.

$H = 15$ cm. The results indicate that at $\Delta T = 10°C$ substantial change in the oscillation amplitude with the location exists. At the cavity center $(X, Y, Z) = (0, 0, 0)$ the flow is nearly steady. The temperature oscillation intensifies as the flow moves towards the isothermal side walls. In spite of the large change in the oscillation amplitude, the flow at all detected locations oscillates periodically with time at the same frequency. Specifically, the signals are characterized by a high frequency small amplitude oscillation superimposed on a low frequency high amplitude oscillation. However, for a lower thermal buoyancy at $\Delta T = 4.6°C$ the flow is nearly steady and the oscillation amplitude depends only slightly on the location (Fig. 8(b)). Checking the data for a higher rotation rate showed that the dependence of the oscillation amplitude on the space coordinates is weaker for $\Omega \geqslant 97.4$ rpm. Typical results are provided in Fig. 9 for $\Omega = 97.4$ and 307.9 rpm with $\phi = 75°$ and $\Delta T = 10°C$. Note that except at the cavity center the

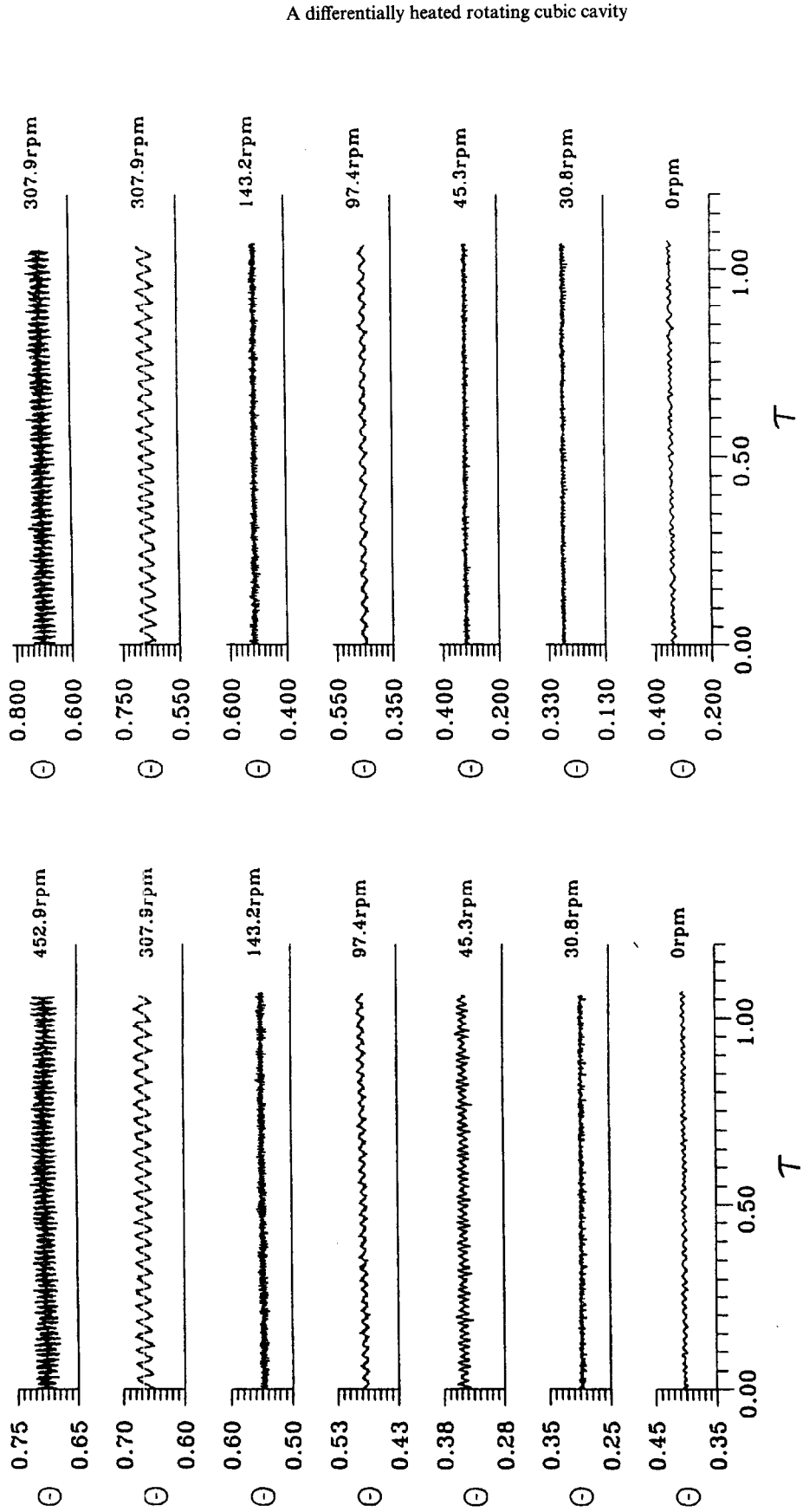

Fig. 6. Measured time records of air temperature at location $X = 0.44$, $Y = 0$ and $Z = 0$ for $\phi = 0°$ and $H = 15$ cm at various rotation rates for: (a) $\Delta T = 10°C$ ($Ra = 3.18 \times 10^6$); and (b) $\Delta T = 4.6°C$ ($Ra = 1.46 \times 10^6$).

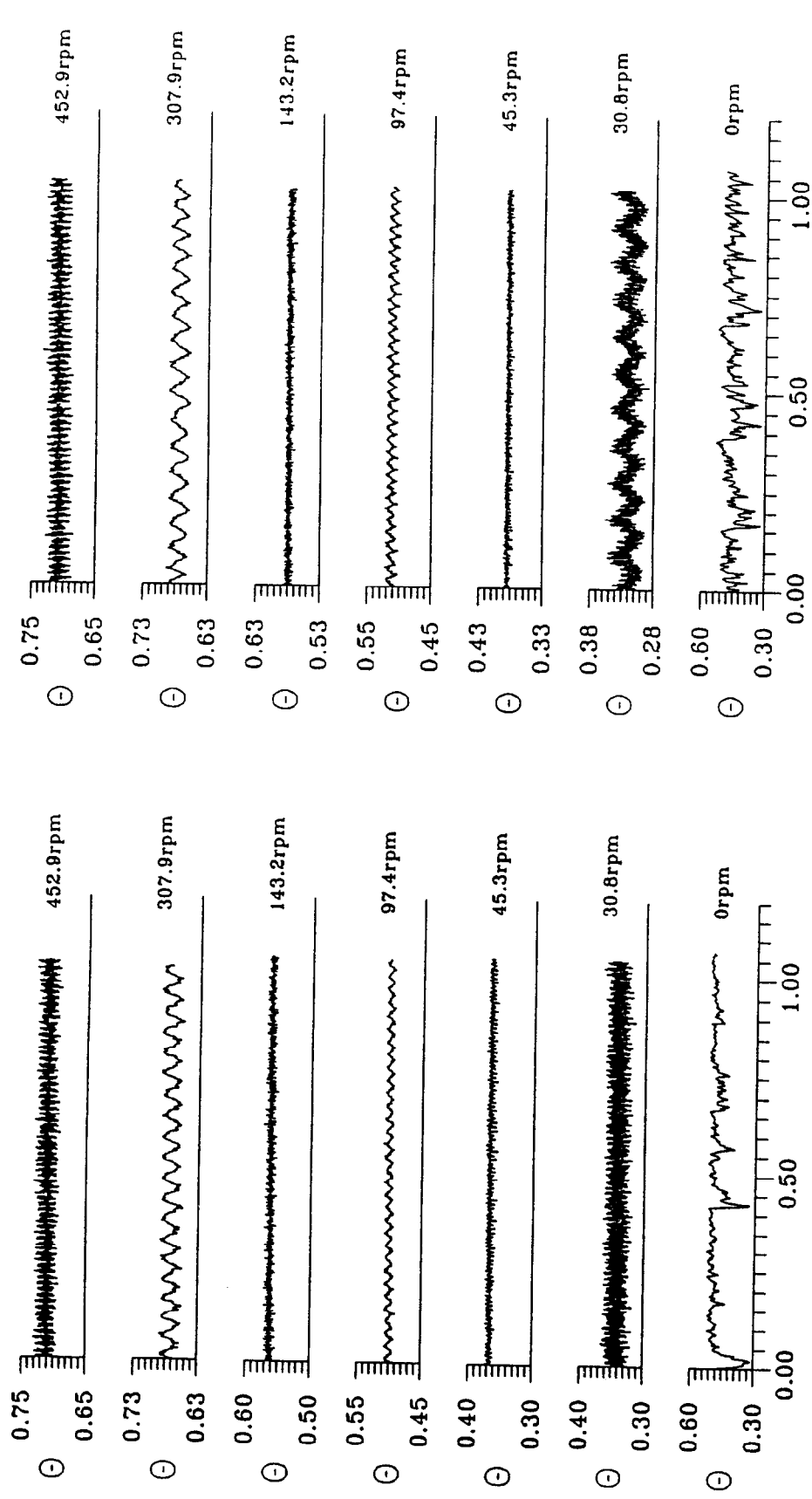

Fig. 7. Measured time records of air temperature at location $X = 0.44$, $Y = 0$ and $Z = 0$ for $H = 15$ cm and $\Delta T = 10°C$ ($Ra = 3.18 \times 10^6$) at various rotation rates for: (a) $\phi = 60°$ and (b) $\phi = 75°$.

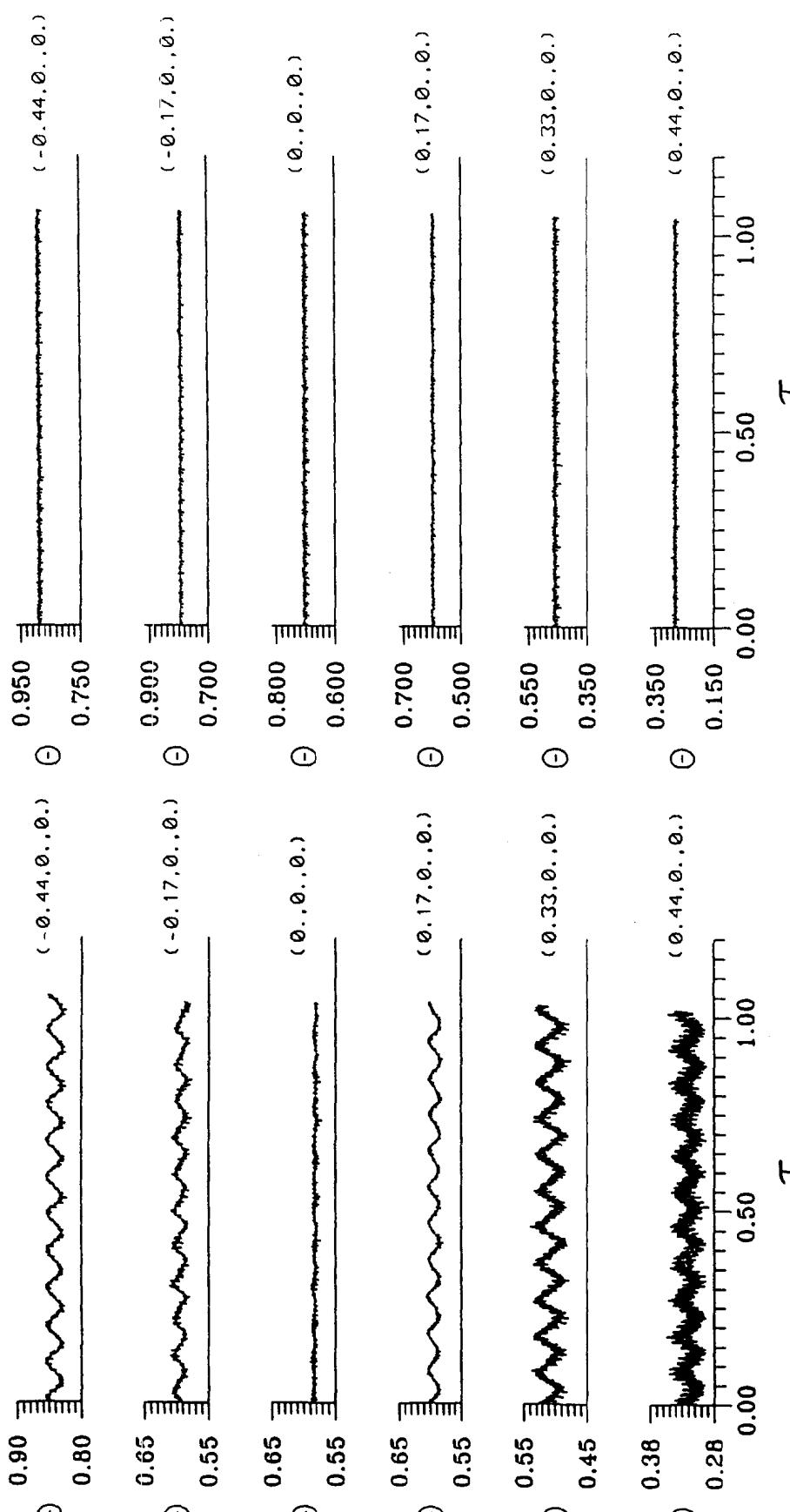

Fig. 8. Measured time histories of air temperature at various locations for $\phi = 75°$, $H = 15$ cm and $\Omega = 30.8$ rpm ($Ta = 2.34 \times 10^7$) for: (a) $\Delta T = 10°C$ ($Ra = 3.18 \times 10^6$, $Ra_\Omega = 5.06 \times 10^5$); and (b) $\Delta T = 4.6°C$ ($Ra = 1.46 \times 10^6$, $Ra_\Omega = 2.34 \times 10^5$).

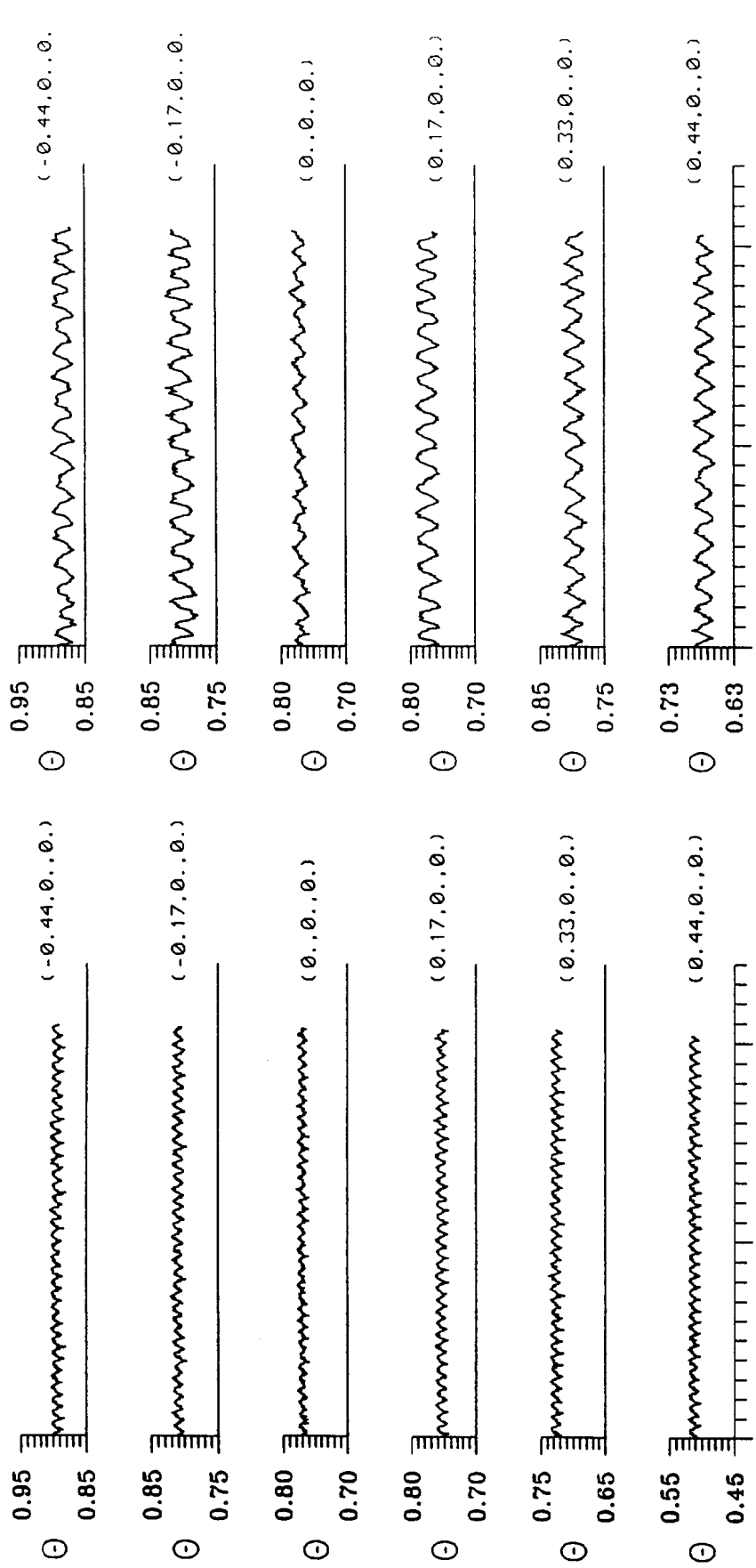

Fig. 9. Measured time histories of air temperature at various locations for $\phi = 75°$, $H = 15$ cm and $\Delta T = 10°C$ ($Ra = 3.18 \times 10^6$) for: (a) $\Omega = 97.4$ rpm ($Ta = 2.34 \times 10^8$, $Ra_\Omega = 5.06 \times 10^6$); and (b) $\Omega = 307.9$ rpm ($Ta = 2.34 \times 10^9$, $Ra_\Omega = 5.06 \times 10^7$).

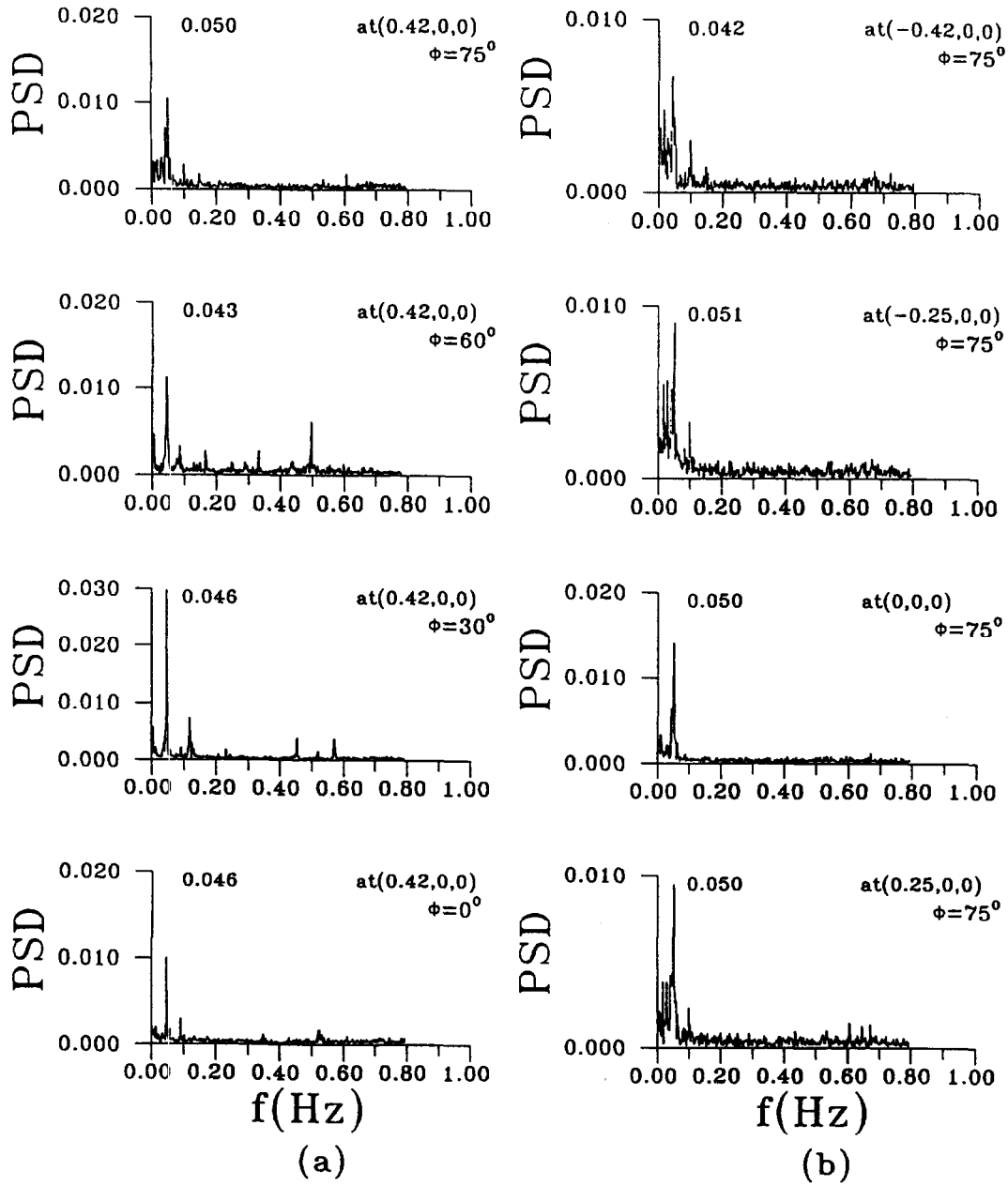

Fig. 10. Power spectrum densities at $\Omega = 97.4$ rpm, $\Delta T = 10°C$ and $H = 10$ cm ($Ra = 9.43 \times 10^5$, $Ta = 4.62 \times 10^7$, $Ra_\Omega = 1 \times 10^6$) for: (a) various inclined angles at location $X = 0.42$, $Y = 0$ and $Z = 0$; and (b) various locations at $\phi = 75°$.

flow oscillates at nearly the same amplitude and frequency. The oscillation amplitude at the cavity center is slightly lower than that at other locations.

To further illustrate the characteristics of the flow oscillation, the power spectrum densities of the measured time histories were obtained by a fast Fourier transform analysis. The results in Fig. 10 for $\Omega = 97.4$ rpm, $\Delta T = 10°C$ and $H = 10$ cm for various inclined angles and locations indicate that the effects of the cavity inclination and spatial position on the dominant oscillation frequency are small for these cases. However, the change in the oscillation amplitude with the angle and position is noticeable, as already shown in Figs. 6–8. Moreover, at a lower rotation rate of 45.3 rpm, Fig. 11(a) shows that there is a slight shift toward a higher oscillation frequency when the inclined angle ϕ is raised from 0 to 90°. Figure 11(b) also shows that the frequency is independent of the space location. A scrutiny of the values of peaks in the plots for the power spectrum densities in Fig. 11 reveals that for these cases the flow oscillation is quasi-periodic and is characterized by two incommensurate

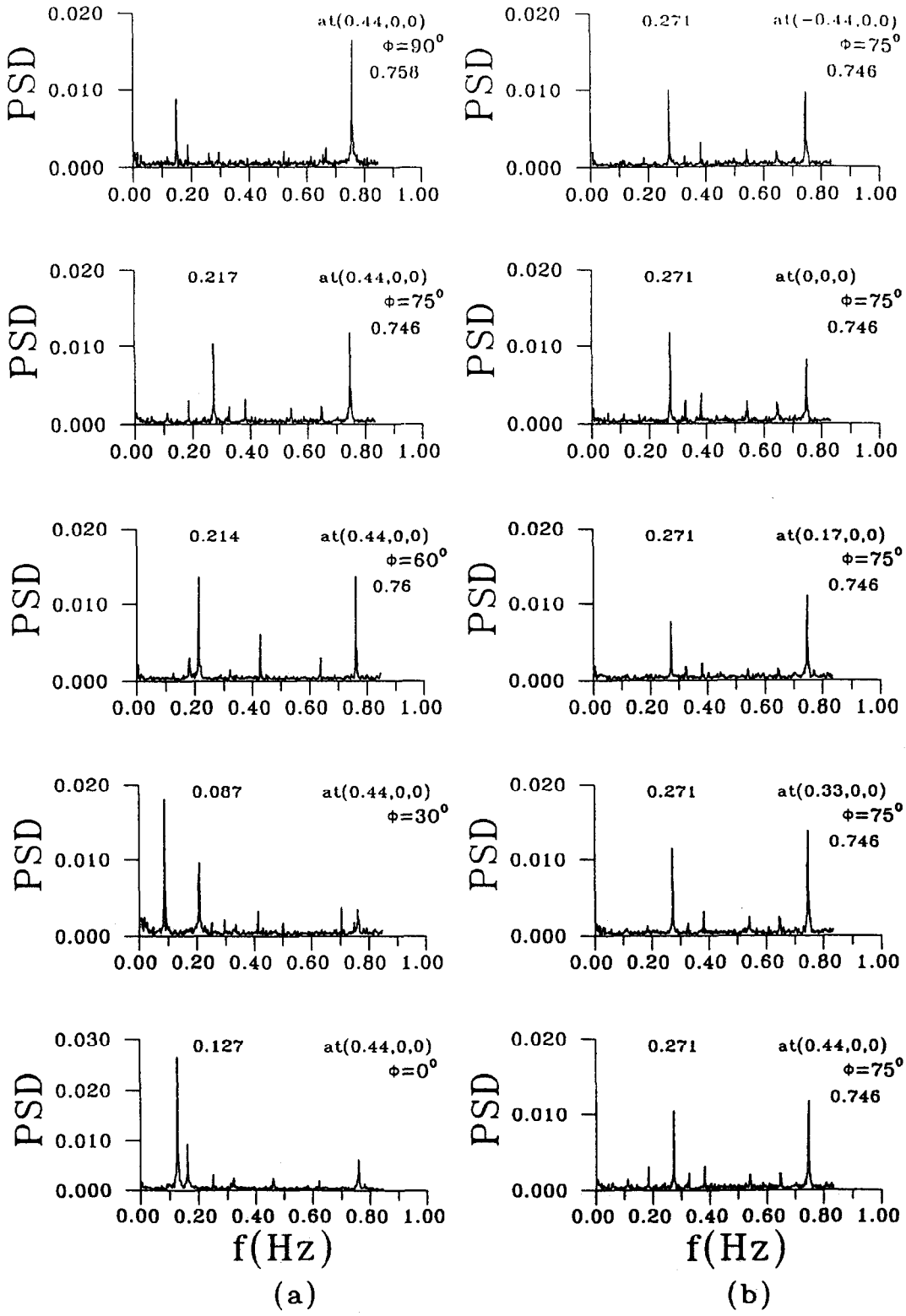

Fig. 11. Power spectrum densities at $\Omega = 45.3$ rpm, $\Delta T = 10°C$ and $H = 15$ cm ($Ra = 3.18 \times 10^6$, $Ta = 2.34 \times 10^8$, $Ra_\Omega = 5.06 \times 10^6$) for: (a) various inclined angles at location $X = 0.44$, $Y = 0$ and $Z = 0$; and (b) various locations at $\phi = 75°$.

fundamental frequencies [21]. For the inclined angle $\phi = 75°$ the two frequencies are 0.271 and 0.746 in Fig. 11(b).

4. CONCLUDING REMARKS

Through detailed experimental measurements of the time-average and instantaneous temperatures in a differentially heated air cavity, the effects of rotation rate and inclined angle on the temporal stability of the flow was investigated in the present study. Data for the time-averaged temperature suggest that the temperature distributions in the X-direction for various inclined angles become widely separate only at low rotation rates, $\Omega < 97.4$ rpm. Flow re-stabilization characterized by the presence of the two different ranges of the rotation rates for the steady flow to prevail was clearly shown from the data for the time records of the air temperature. The flow re-stabilization is more pronounced at a high inclined angle. Moreover, for a given temperature difference, rotation rate and inclined angle the oscillation amplitude of the air temperature depends significantly on the location in the cavity at a low Ω. However, the oscillation frequency is the same.

During the course of this investigation it is noted that the effects of rotation on the stabilization of the cavity flow are especially important in the cylindrical geometry as far as the growth of bulk crystal for the semiconductor application is concerned. These effects will be explored in the near future.

Acknowledgement—The financial support of this study by the engineering division of National Science Council of Taiwan, Republic of China through the contract NSC 83-0401 E-009-009 is greatly appreciated.

REFERENCES

1. Lee, T. L. and Lin, T. F., Transient three-dimensional convection of air in a differentially heated rotating cubic cavity. *International Journal of Heat and Mass Transfer*, 1996, **39**, 1243–1255.
2. Ker, Y. T. and Lin, T. F., A combined numerical and experimental study of air convection in a differentially heated rotating cubic cavity. *International Journal of Heat and Mass Transfer*, 1995, **39**, 3193–3210.
3. Niller, P. P. and Bisshopp, F. E., On the influence of Coriolis force on onset of thermal convection. *Journal of Fluid Mechanics*, 1965, **22**, 753–761.
4. Veronis, G., Large-amplitude Bënard convection in a rotating fluid. *Journal of Fluid Mechanics*, 1968, **31**, 113–139.
5. Küppers, G. and Lortz, D., Transition from laminar convection to thermal turbulence in a rotating fluid layer. *Journal of Fluid Mechanics*, 1969, **35**, 609–620.
6. Rossby, H. T., A study of Bënard convection with and without rotation. *Journal of Fluid Mechanics*, 1969, **36**, 309–335.
7. Hunter, C. and Riahi, N., Nonlinear convection in a rotating fluid. *Journal of Fluid Mechanics*, 1975, **72**, 433–454.
8. Rudraiah, N. and Chandna, O. P., Effects of Coriolis force and nonuniform temperature gradient on the Rayleigh–Bënard convection. *Canadian Journal of Physics*, 1986, **64**, 90–99.
9. Clever, R. M. and Busse, F. H., Nonlinear properties of convection rolls in a horizontal layer rotating about a vertical axis. *Journal of Fluid Mechanics*, 1979, **94**, 609–627.
10. Hudson, J. L., Tang, D. and Abell, S., Experiments on centrifugal driven thermal convection in a rotating cylinder. *Journal of Fluid Mechanics*, 1978, **86**, 147–159.
11. Tang, D. and Hudson, J. L., Experiments on a rotating fluid heated from below. *International Journal of Heat and Mass Transfer*, 1983, **26**, 943–949.
12. Chew, J. W., Computation of convective laminar flow in rotating cavities. *Journal of Fluid Mechanics*, 1985, **153**, 339–360.
13. Buell, J. C. and Catton, I., Effect of rotation on the stability of a bounded cylindrical layer of fluid heated from below. *Physical Fluids*, 1983, **26**, 892–896.
14. Pfotenhauer, J. M., Niemela, J. J. and Donnelly, R. J., Stability and heat transfer of rotating cryogens. Part 3. Effects of finite cylindrical geometry and rotation on the onset of convection. *Journal of Fluid Mechanics*, 1987, **175**, 85–96.
15. Boubnov, B. M. and Golitsyn, G. S., Experimental study of convective structures in rotating fluid. *Journal of Fluid Mechanics*, 1986, **167**, 503–531.
16. Kirdyashkin, A. G. and Distanov, V. E., Hydrodynamics and heat transfer in a vertical cylinder exposed to periodically varying centrifugal forces (accelerated crucible rotation technique). *International Journal of Heat and Mass Transfer*, 1990, **33**, 1397–1415.
17. Abell, S. and Hudson, J. L., An experimental study of centrifugally driven free convection in rectangular cavity. *International Journal of Heat and Mass Transfer*, 1975, **18**, 1415–1423.
18. Hathaway, D. H. and Somerville, R. C. J., Three-dimensional simulations of convection in layers with tilted rotation vectors. *Journal of Fluid Mechanics*, 1983, **126**, 75–89.
19. Bühler, K. and Oertel, H., Thermal cellular convection in rotating rectangular boxes. *Journal of Fluid Mechanics*, 1982, **114**, 261–282.
20. Lee, T. L. and Lin, T. F., Three-dimensional natural convection of air in an inclined cubic cavity. *Numerical Heat and Mass Transfer*, 1995, **27**, 681–703.
21. Argyris, J., Faust, G. and Haase, M., An adventure in chaos. *Computational Methods in Applied Mechanics and Engineering*, 1991, **91**, 997–1091.